3. J. F. Wehner and R. H. Wilhelm, Chem. Eng. Sci., 6, 89 (1956).
4. A. Kneschke, Differentialgleichungen, Vol. 1, Teubner Verlagsgesellschaft, Leipzig (1965).

THE DYNAMIC PRESSURE FROM A COMPRESSED ARC IN METAL CUTTING

V. G. Davydenko and V. D. Shimanovich

UDC 621.791

Direct spectroscopic techniques applied to plasma metal cutting show that the dynamic pressure is dependent on the working conditions in the plasma source.

The metal melts during plasma cutting mainly in the zone of the periodically moving anode spot; the molten metal is transported by the hot gas, and it is therefore important to examine the dynamic pressure exerted by the flow in relation to source conditions in order to choose the optimum cutting conditions [1]. The dynamic characteristics have been examined [2] by means of contact transducers in a system where the metal was a water-cooled copper disk. More reliable determinations have been provided by optical spectroscopy, since these provide much higher time resolution.

We used the system of [1], which contained a power supply and an OPR-11 control unit, as well as a PMR-6 plasma source, where the workpiece was a strip of Kh18N10T steel of thickness 10-50 mm. The range of working conditions was as follows: current I = 150-300 A, voltage U = 165-200 V, gas flow rate (nitrogen) R_g = 50-125 liters/min, diameter of cathode nozzle d_c = 2.5-3.5 mm, and length of open zone of plasma h = 6 mm.

The data of [1] were used to determine the dynamic head ρV^2 (where ρ is density and V is velocity) from the velocity V averaged over the cross section and spectroscopic measurement of the temperature, which is required in order to calculate ρ. The spectra were recorded photographically with an ISP-30. The region 300-565 nm from the open plasma consists of a continuum and the lines from nitrogen atoms and ions (Fig. 1). Spectral lines due to the electrodes (cathode and anode) are absent. This means that the open zone can be treated as free from impurities, so spectroscopic techniques can be used to determine the temperature from the nitrogen line strengths on the assumption that the plasma consists of nitrogen only. The transparent-plasma approximation was used with the NII 359.3 and 504.5 nm lines, which show no reabsorption under these conditions [3, 4]. The correction was applied for the plasma nonuniformity by solving Abel's integral equation by the method of [5] (NII 359.3; 360.9; 391.9; 517.5 nm); the plasma composition and the transition probabilities were taken from [6, 7, 9]. The relative error in determining the temperature from the absolute intensities did not exceed 5%.

Figure 2 shows the radial temperature distributions at 2 mm from the end of the nozzle for a nitrogen flow rate of 50 liters/min for discharge currents of 150, 200, 250, and 300 A; the plasma had a higher temperature gradient. The maximum temperature attained under these conditions was 19,000°K for I = 200 A; then the temperature at 1.5 mm from the axis was 14,000°K. It was difficult to measure the temperature at more remote points on account of the poor dynamic range in the photographic recording. In addition, the central ray was used to determine the temperature from the relative intensities of the NII 359.3, 360.9, 391.9, and 517.5 nm lines. The discrepancy between the axial temperature and the temperature from the central ray was less than 3000°K.

These results do not agree with those of [8], where a rise in axial temperature with arc current was reported. The temperature attained 30,000°K for I = 300 A. Possible reasons for the discrepancy are as follows. First, the rise in axial temperature with the current was slight and lay within the error of experiment, and the workpiece was replaced [8] by a water-cooled anode, which could affect the plasma parameters. Also, the system had a poor

Physics Institute, Academy of Sciences of the Belorussian SSR, Minsk. Translated from Inzhenerno-Fizicheskii Zhurnal, Vol. 34, No. 4, pp. 684-689, April, 1978. Original article submitted April 7, 1977.

0022-0841/78/3404-0461$07.50

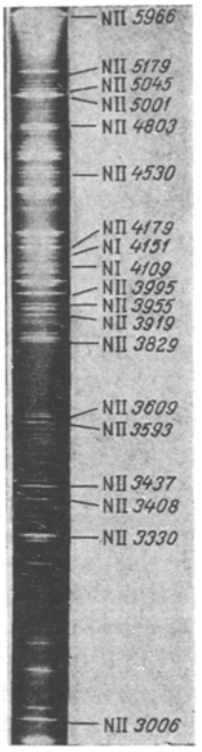

Fig. 1. Emission spectrum of plasma jet, I = 200 A, U = 165 V, R_g = 50 liters/min, d_c = 2.5 mm.

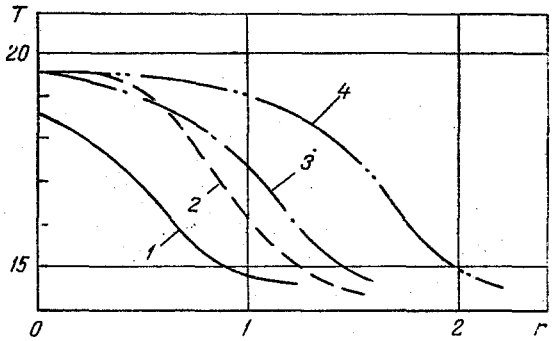

Fig. 2. Radial temperature distributions in plasma jet (R_g = 50 liters/min, d_c = 2.5 mm): 1) I = 150 A; 2) 200; 3) 250; 4) 300, r in mm; T in 10^3°K.

spectral resolution, as is clear from the spectrogram of [8]. Finally, it was impossible [8] to determine the intensity of the NII 517.9 nm line reliably, since the adjacent NII 518.6 and 519.0 nm lines overlapped it. This resulted in a considerable overestimate of the NII 517.9 nm intensity and thus of the temperature.

Our temperature measurements and the data of [1] were used to determine the dynamic head for the studied working regimes of the plasma jet (Table 1); the gas flow rate was constant at 50 liters/min. It was assumed that the plasma density was $\rho = m_{NI}(n_{NI} + n_{NII} + n_{NIII})$ where m_{NI} is the mass of the nitrogen atom and n_{NI}, n_{NII}, and n_{NIII} are the concentrations of the corresponding species. Table 1 shows that the dynamic head increases by about a factor of 2 between 150 and 300 A, which substantially exceeds the error of experiment.

These results do not agree with the data of [2], where the measurements were made with contact transducers. For instance, our speeds for the corresponding working conditions are

TABLE 1. Dynamic Head in Plasma Jet as a Function of Discharge Current for R_g = 50 Liter/Min

I, A	d_c, mm	Mean T, °K	V, m/sec	ρV^2, g/cm·sec^2
150	2,5	$18{,}5 \cdot 10^3$	$0{,}9 \cdot 10^3$	$1{,}7 \cdot 10^4$
200	2,5	$19{,}5 \cdot 10^3$	$1 \cdot 10^3$	$2{,}1 \cdot 10^4$
250	3	$19{,}5 \cdot 10^3$	$1{,}2 \cdot 10^3$	$2{,}5 \cdot 10^4$
300	3	$19{,}5 \cdot 10^3$	$1{,}3 \cdot 10^3$	$3{,}6 \cdot 10^4$

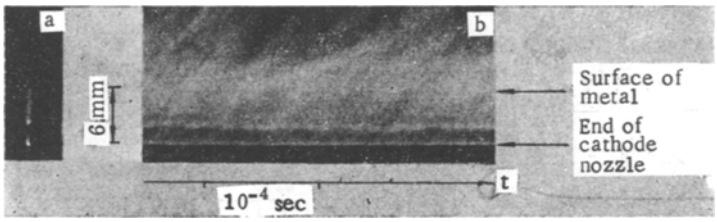

Fig. 3. a) Photograph ($\tau = 2 \cdot 10^{-4}$ sec) b) SFR camera recording ($\tau = 10^{-6}$ sec) on plasma jet, magnification ×2, sweep speed 375 m/sec. I = 200 A, U = 185 V, R_g = 125 liters/min, d_c = 2.5 mm.

almost half the others. This may be due to the considerable difference in time resolution between our devices and those of [2].

We also examined the scope for increasing the dynamic pressure by raising R_g; we found that flow rates above 50 liters/min caused the plasma jet to vary along its length, since an intensely emitting zone arose at the nozzle, which moved away from the latter as the flow rate increased. A very interesting pattern was observed at the maximum flow rate of 125 liters/min with I = 200 A and d_c = 2.5 mm; Fig. 3 shows a photograph (exposure time $2 \cdot 10^{-3}$ sec) and part of an SFR camera recording made with a time resolution of 10^{-6} sec by the metho of [1]. In both cases, there are clearly three characteristic zones: the dark space, a shoc wave, and a region at the surface of the workpiece.

The high-speed scans showed that the plasma jet produced periodic microbunches moving at speeds in excess of 1 km/sec towards the anode (Table 2). The frequencies of these bunches were respectively 180 and 360 kHz at flow rates of 50 and 125 liters/min, while the characteristic dimensions of the bunches were 1 and 0.2 mm. A compressed arc is a set of moving plasma bunches, so the shock wave on the photograph is the average result of the waves recorded with the SFR camera.

Table 3 gives estimates of the plasma parameters derived spectroscopically; the temperature was determined from the relative intensity of the NII 504.5 and NII 391.9 nm lines. The transverse pattern in the emission intensities causes considerable error when the relative intensities are employed, so we determined the temperature from the intensities averaged over the cross section for the central ray. This method was also used in determining the electron concentration from the absolute intensity of the continuum at 495.5 nm [10]. The pressures in the various parts of the discharge were estimated in this way, and we found that the maximum pressure (5.5 atm) occurred at the shock wave, while the pressure at the surface of the metal was atmospheric.

The most likely cause of the nonuniformity along the jet is that the supersonic flow does not have time to expand fully at high gas flow rates. The current, the flow rate, and the nozzle diameter determine the distance l from the end of the nozzle at which the shock wave arises. The time-averaged value is l = 2 mm for a flow rate of 25 liters/min, while it has been claimed [11] that l for a nitrogen plasma is defined by

$$\frac{P_0}{P_\infty} = 2.4 \left(\frac{l}{d_c} \right)^2, \qquad (1)$$

where P_0 and P_∞ are the pressures in the source and in the surroundings, respectively.

The following assumptions are made in deriving this expression:

1. The static pressure at the shock wave is approximately equal to the surrounding pressure.

TABLE 2. Effects of Nitrogen Flow Rate on Plasma Parameters

R_g, liters/min	I, A	U, V	Pulsation frequency f (kHz) of plasma microbunches	Visible diameter d (mm) of plasma jet for time resolution of		Length b of plasma bunch, mm
				$2 \cdot 10^{-3}$ sec	10^{-4} sec	
50	200	165	180	3	1	1
125	200	185	360	0,6	0,2	0,2

TABLE 3. Plasma Parameters in Various Discharge Zones for Maximum Gas Flow Rate R_g of 125 liters/min

Discharge zone	T, °K	n_e, cm^{-3}	P, atm	ρ, g/cm^3	V, m/sec	ρV^2, $g/cm \cdot sec^2$
Before shock wave	30000 ± 4000	$4 \cdot 10^{17}$	3	$7 \cdot 10^{-6}$	1200	$5 \cdot 10^4$
In shock wave	29000 ± 4000	$6 \cdot 10^{17}$	5	—	—	—
At surface of metal	23000 ± 3000	$1{,}4 \cdot 10^{17}$	1	$3{,}4 \cdot 10^{-6}$	1200	$6 \cdot 10^6$

2. The flow along the jet is analogous to adiabatic one-dimensional flow in a nozzle. In our case, the first assumption is confirmed by the pressure determination at the surface of the metal (Table 3).

From (1) we get for our conditions (flow rate 125 liters/min, 200 A, time-averaged l = 2 mm) that P_0 = 4 atm; the SFR recording indicates that l pulsates with a frequency of 360 kHz within limits of 0.3 mm, which (1) indicates as implying a periodic pressure variation in the shock wave in the range 3-5 atm.

The parameters given in Table 3 relate to the plasma bunches arising periodically in the steady-state supersonic flow; the temperature and flow speed must be less than these bunch parameters. The spectra of the various zones also indicate that the temperature in the supersonic flow should be well below the bunch temperature. An estimate was made on the assumption that $V_{flow} \approx V_{bunch}$ = 1.2 km/sec, which gave an upper bound to the flow temperature of T_u = 4000°K.

The following conclusions are drawn:

1. A compressed plasma arc as used in cutting metals is a steady-state flow containing periodic high-speed hot plasma bunches. The steady-state flow may be supersonic at high flow rates.

2. Spectroscopic temperature measurement and speed measurement from time scans show that the flow consists mainly of plasma bunches.

3. The dynamic head increases with the discharge current and is almost independent of the gas flow rate.

NOTATION

I, current; U, voltage; ρ, plasma density; V, flow velocity; R_g, gas flow rate; m_{NI}, mass of nitrogen atom; n_{NI}, n_{NII}, n_{NIII}, atom and ion concentrations; d_c, nozzle diameter; ρV^2, dynamic head; τ, exposure time; P_0, pressure in receiver; P_∞, ambient pressure; l, distance from nozzle to shock wave; b, length of plasma microbunch.

LITERATURE CITED

1. V. G. Davydenko, E. P. Kharitonov, I. S. Shapiro, and V. D. Shimanovich, Inzh.-Fiz. Zh., 2, No. 3 (1974).
2. S. V. Alekseev et al., "A study of the speed and temperature in a high-intensity compressed arc in nitrogen and argon," in: Physics, Technology, and Applications of Low-Temperature Plasmas [in Russian], Alma-Ata (1970), p. 145.
3. D. G. Bykhovskii, Plasma Cutting [in Russian], Moscow (1972), p. 8.

4. V. M. Batenin and P. V. Minaev, Teplofiz. Vys. Temp., 7, No. 2 (1969).
5. W. Pierce, in: Production and Examination of High-Temperature Plasma [Russian translation], IL, Moscow (1962).
6. W. Wiese and M. Smith, Atomic Transition Probabilities (1966).
7. J. Burchorn, Z. Phys. Chem., No. 3, 215 (1960).
8. J. Takakija and K. Takaynki, IEEE Trans. Ion and Gas Applic., No. 6 (1970).
9. S. V. Dresvin (editor), Physics and Technology of Low-Temperature Plasmas [in Russian] (1972).
10. L. M. Biberman and G. N. Norman, Usp. Fiz. Nauk, 91, 193 (1967).
11. Christ, Sherman, and Glass, Raketn. Tekh. Kosmonavt., No. 1 (1966).

ON THE THEORY OF THE EQUATION OF STATE OF REAL GASES. II

V. A. Bubnov

UDC 536.711

A comparison is made between the equation of state derived earlier and experiment.

4. INITIAL THEORETICAL FORMULAS

It was shown in the previous paper that the computation of triple, quadruple, etc. collisions is equivalent to the introduction of correlations between statistical criteria into the statistics, for which the thermal velocity components were taken. If we go from the correlation coefficient r over to the complex n = r/(1 + r), then the equation of state we obtained has the form

$$\frac{pv}{RT} = \Psi(n) - B\rho, \tag{29}$$

where

$$\left.\begin{aligned} \Psi(n) &= \frac{1-n}{(1+n)(1-2n)} \\ n &= \sqrt{\rho}(A_1 + A_2\rho) \end{aligned}\right\}, \tag{30}$$

$$\left.\begin{aligned} A_1 &= 0.8096\cdot 10^{-2} + 0.4481\cdot 10^{-2}\frac{T_k}{p_k} \\ A_2 &= 0.9924\cdot 10^{-5} - 0.5481\cdot 10^{-5}\frac{T_k}{p_k} \end{aligned}\right\}. \tag{31}$$

Comparing (29) with experimental results can clarify the constant B, and a clarification of the nature of the interaction forces between the molecules can thereby be made. The peculiarity of the viewpoint elucidated is the separation of the virial of the internal forces from the factors due to triple, quadruple, etc. collisions. If we turn to the usual description of the equation of state in terms of the virial coefficients, then the latter, found by using experimental data, contain not only what results from the interaction force, but also what is due to multiple collisions. And this means execution of a logical error and obtaining distorted information about the nature of the molecular interaction forces.

5. ON THE EQUATION OF STATE OF ARGON

We used the Michels measurements [1] for argon in which the pressure varied between 1 and 2900 atm and the temperature between 50 and 100°C. In order to conserve a high degree of measurement accuracy, the density in the Michels tests was expressed in Amag units (one Amag unit of the density equals $4.4636\cdot 10^5$ mole/cm^3).

The density is also defined in these units in our computations. For argon $T_k/P_k = 3.125$; then we have according to (31): $A_1 = 0.2210\cdot 10^{-1}$, $A_2 = -0.7204\cdot 10^{-5}$, which in turn determines the dependence of n on the density:

Moscow Instrument and Tool Institute. Translated from Inzhenerno-Fizicheskii Zhurnal, Vol. 34, No. 4, pp. 690-696, April, 1978. Original article submitted February 8, 1977.

0022-0841/78/3404-0465$07.50